Monatshefte für Chemie 136, 1885–1897 (2005)
DOI 10.1007/s00706-005-0388-6

Monatshefte für Chemie
Chemical Monthly
Printed in Austria

Fractional Site Occupation in Ternary Metal Compounds: Structure, Bonding, and Thermodynamics[#]

Klaus W. Richter*

Department of Inorganic Chemistry – Materials Chemistry, University of Vienna, A-1090 Wien, Austria

Received September 12, 2004; accepted December 14, 2004
Published online November 14, 2005

Summary. Ternary compounds of the type $(M,M')_xA_y$ where M and M' are early transition metals of the groups 4–6 and A is a main group element of the groups 14–16 are showing interesting substitution mechanisms among the metal atoms ranging from classical and partially ordered solid solution phases to ternary compounds showing differential fractional site occupation. In these compounds the transition metals show mixed site occupation at the metal positions in combination with pronounced site preferences leading to varying metal mixtures at crystallographically independent sites. The connection between partial ordering and the differences in the local coordination of the respective lattice sites is discussed. Chemical bonding arguments obtained from electronic calculations using the extended *Hückel* approach are used to understand the observed distribution of the metals over the respective lattice sites and allow a qualitative prediction of site preferences. A thermodynamic model was applied in order to investigate the observed substitution mechanism and *Gibbs* energies for the occupation of the lattice sites with different metal atoms could be obtained by adjusting the model parameters to the experimentally observed site fractions.

Keywords. Transition metal compounds; Substitution; Differential fractional site occupation; Crystal structure; Electronic structure.

Introduction

Compounds of the early transition metals M (groups 4 to 6 of the periodic table) with p-block elements of the groups 14 to 16 (A) generally show a rich and interesting chemistry and a great variety of stoichiometries and crystal structures are found in these systems [1]. It is not obvious that the addition of a second early transition metal M' to a M–A system will yield the formation of new ternary compounds. As all early transition metal atoms are rather similar in their basic

* Corresponding author. E-mail: klaus.richter@univie.ac.at
[#] Dedicated to Prof. *Adolf Mikula* on the occasion of his 60th birthday

properties like size or electronegativity, one might predict the formation of extended solid solutions in the binary compounds rather than new ternary compounds with crystal structures differing form those observed in the binaries.

The formation of a ternary solid solution phase $(M,M')_xA_y$ in its simplest form would yield an undisturbed *A*-sublattice and a completely random mixture of *M* and *M′* at the metal sublattice yielding entropic stabilization of these phases. However, as most of the compounds M_xA_y exhibit complicated crystal structures, they usually cannot be described by one single metal sublattice, but rather by a varying number of crystallographically independent metal sites. Each independent metal site exhibits its own characteristic local coordination, so the local ''site properties'' may vary substantially from site to site. In terms of substitution by an additional metal this opens up the opportunity for differentiation, and thus the possibility of preferred site occupation. As a consequence, a partially ordered solid solution may form instead of a completely random solid solution. Furthermore it is possible that new ternary compounds are formed rather than solid solutions. These compounds combine mixed site occupations at the metal sites with pronounced site preferences, i.e., strong variations of the fractional site occupations observed at crystallographically independent sites.

In fact, a steadily increasing number of such ternary compounds $(M,M')_xA_y$ were synthesized and structurally characterized within the last two decades. A compilation and discussion of structural features and stabilization of ternary mixed early transition metal pnictides and chalcogenides was recently given by *Kleinke* [2] and includes a series of Nb–Ta sulfides [3–7] and mixed group 4-group 5 sulfides [8, 9] as well as various mixed pnictides [10–19].

Site Preferences and their Rationalization

In a series of papers in the early 1990s, *Franzen et al.* reported on the synthesis and characterization of four mixed Nb–Ta sulfides: $Nb_{4.92}Ta_{6.08}S_4$ [3], $Nb_{6.74}Ta_{5.26}S_4$ [4], $Nb_{1.72}Ta_{3.28}S_2$ [5], and $Nb_{0.95}Ta_{1.05}S$ [6] with unique crystal structure types not found in either of the adjacent binary systems. Their common structural features led to the chemical concept of *Differential Fractional Site Occupation* (DFSO) [20] which outlines the special features of a whole series of ternary compounds $(M,M')_xA_y$ observed since then. These common features are: 1) the metal atom sites are occupied by mixtures of *M* and *M′* randomly distributed over a given set of equivalent sites; 2) the fractional occupancies of the sites are rather narrowly fixed for each site but vary substantially from site to site; and 3) the structures of the ternaries are not found in either of the corresponding binary systems.

As an example for DFSO consider the compound $Nb_{2.73}Ta_{4.27}S_2$ (*oP*36, *Pnma*) which was recently synthesized by *Debus* and *Harbrecht* [7]. The crystal structure of this compound is shown in Fig. 1 and consists of distorted M_{13} icosahedral clusters which are condensed into pentagonal antiprismatic columns parallel to the *a*-axis of the orthorhombic structure. Of the five crystallographically independent metal sites, four are occupied by mixtures of Ta and Nb with occupation factors between 23 and 71% Ta and one is occupied by pure Ta (compare Table 1).

The stabilization of $Nb_{2.73}Ta_{4.27}S_2$ by DFSO may be rationalized by the competition between entropic stabilization and small differences in the bonding

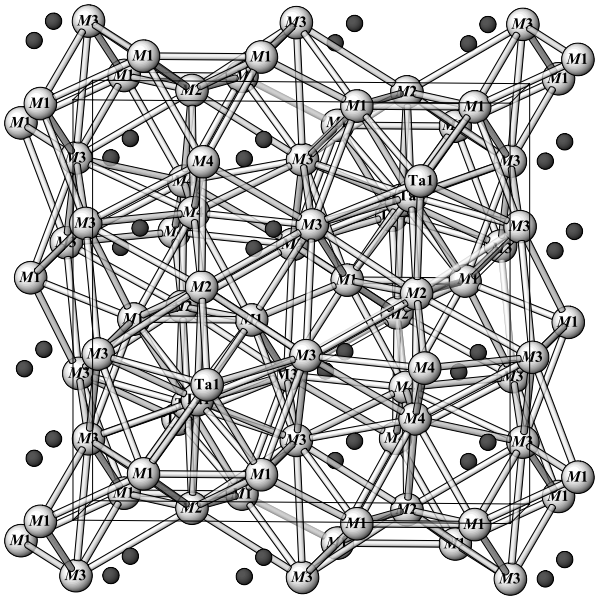

Fig. 1. The crystal structure of $Nb_{2.73}Ta_{4.27}S_2$ [7]; projection along [100]; metal atoms: bright spheres; sulfur atoms: small dark spheres; metal–metal bonds up to a distance of 3.5 Å are shown as sticks; the five independent metal sites are occupied by different mixtures of Nb/Ta (compare Table 1)

Table 1. Site occupation, *Pauling* bond order sums (*P*BO), and cumulated *Mulliken* overlap populations (*M*OP) for all metal sites of $Nb_{2.73}Ta_{4.27}S_2$ according to Ref. [7]

Atom	*y*(Ta)	*P*BO	*M*OP (Nb_7S_2)	*M*OP (Ta_7S_2)
Ta1	1	5.52	3.54	3.86
*M*1	0.71	3.41	2.69	2.96
*M*2	0.74	2.69	2.93	3.20
*M*3	0.43	1.98	2.39	2.62
*M*4	0.23	2.29	2.01	2.23

capability connected with the local coordination at different sites. The entropy term obviously favors mixed site occupation and a maximum stabilizing contribution from the configuration entropy would be reached at a completely even distribution of Ta and Nb over all five metal positions (in this case 61% Ta site fraction at all positions). The observed differentiation of the Ta/Nb substitution clearly points to differences of the bond energies of Ta and Nb at different metal sites promoting the site preferences in order to yield a maximum in total bond energy.

As Nb and Ta virtually have the same size (atomic radius 143 pm, *Pauling* radius 134 pm) [21], it can be ruled out that geometrical size factors are responsible for the observed site preferences. In this case, differences in the capability to form metal–metal bonds were found to be the key for an understanding of site preferences [7]. The larger and more diffuse character of the 5*d*-orbitals of Ta with respect to the 4*d*-orbitals of Nb promotes the ability to form strong metal–metal

bonds. Thus Ta will preferably occupy those lattice sites which, due to their local coordination environment, promote stronger metal–metal interactions. A first approach for a quantitative treatment of this idea for mixed Nb/Ta sulfides was outlined by *Yao et al.* [22] who successfully correlated the site fraction of Ta at a specific lattice site with the *Pauling* bond order n calculated with $D_n = D_1 - 0.6 \log n$ [23] (D_n = bond length, D_1 = sum of *Pauling* radii) summed up for all metal–metal bonds observed at this lattice site. *Mulliken* overlap populations (*M*OP) obtained by extended *Hückel* calculations may also be used as a measure for the extent of metal–metal bonding at a specific site. Both, *Pauling* bond orders as well as *M*OPs obtained by extended *Hückel* calculations have been used by *Debus* and *Harbrecht* [7] for correlation with the experimentally observed site fractions in $Nb_{2.73}Ta_{4.27}S_2$. The respective numerical values as listed in Table 1 show a clear trend for higher Ta occupation at the sites with higher metal–metal interaction.

Figure 2 shows a graphical representation of *M*OPs calculated for the various Nb–Ta-sulfides plotted *versus* the respective fractional site occupations determined by single crystal X-ray diffraction. As it can be seen, a good correlation is observed in any single case, but the curves for different sulfides do not coincide well which is most likely due to the fact that the metal/sulfur ratio and thus the amount of metal–metal interaction varies substantially between the different structures. Site preference effects in mixed Nb/Ta compounds may thus be rationalized by a balanced competition of metal–metal bonding energy and entropic stabilization yielding differential fractional site occupation at the independent metal sites.

The pair Ta–Nb is obviously a unique combination of elements, as the similar radii, number of valence electrons, and electronegativities allow the interpretation of site preferences by a single parameter. All other metal combinations discussed

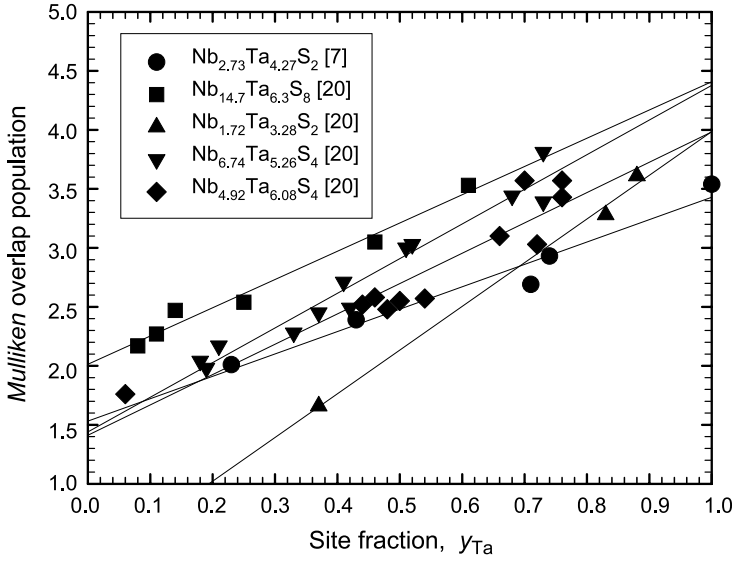

Fig. 2. *Mulliken* overlap populations calculated for various mixed Nb–Ta sulfides (using hypothetical binary Nb-sulfides as model compounds) plotted *versus* experimentally observed site fractions at crystallographically independent lattice sites

here exhibit differences in one or more of the mentioned properties and their site preferences are thus governed by a combination of factors. During our studies we investigated mixed Hf–Nb- and Zr–Ta-germanides in order to gain deeper insight into the driving forces promoting site preferences.

In the Zr–Ta–Ge system, the two phases $Zr_{4-x}Ta_{1+x}Ge_4$ (*mP*18, $P2_1/c$, $U_2Mo_3Si_4$-type) and $Zr_{2+x}Ta_{3-x}Ge_4$ (*oP*36, *Pnma*, Sm_5Ge_4-type) occur adjacent to the solid solution of Ta in binary Zr_5Ge_4, $Zr_{5-x}Ta_xGe_4$ (*tP*36, $P4_12_12$, Zr_5Si_4-type) [24]. The three phases are structurally closely related and form a phase bundle at the M_5Ge_4 stoichiometry. The compound $Zr_xTa_{11-x}Ge_8$ (*oP*76, *Pnma*, $Cr_{11}Ge_8$-type) is stabilized by small amounts of Zr ($0.7<x<1.3$) as well as by Ti- and Hf-additions [25]. The Hf–Nb–Ge system is much simpler and an extended solid solution phase was found to exist at M_5Ge_4 stoichiometry: $Hf_{5-x}Nb_xGe_4$ (*oP*36, *Pnma*, Sm_5Ge_4-type) with $0\leq x\leq 3.8$. This phase combines a large solid solubility range with strong site preferences leading to an almost stepwise substitution mechanism at the metal sites [26].

The Sm_5Ge_4-type structure adopted by $Hf_{5-x}Nb_xGe_4$ as well as by $Zr_{2+x}Ta_{3-x}Ge_4$ is shown in Fig. 3. The structure can be described by a combination of two principal building blocks: trigonal prisms of metal atoms centered by the main group element (Ge) and bcc-type fragments (distorted metal cubes centered by a metal atom). The two building blocks are condensed to infinite slabs stacked alternately in the [010] direction. The three independent metal sites of the structure type shown in Fig. 3 reveal considerable differences in their local coordination with coordination numbers 14 (*M*1), 16 (*M*2), and 17 (*M*3). The close structural relations with monoclinic $Zr_{4-x}Ta_{1+x}Ge_4$ and tetragonal $Zr_{5-x}Ta_xGe_4$ have already been discussed [24]. All three phases are formed from the same principal building

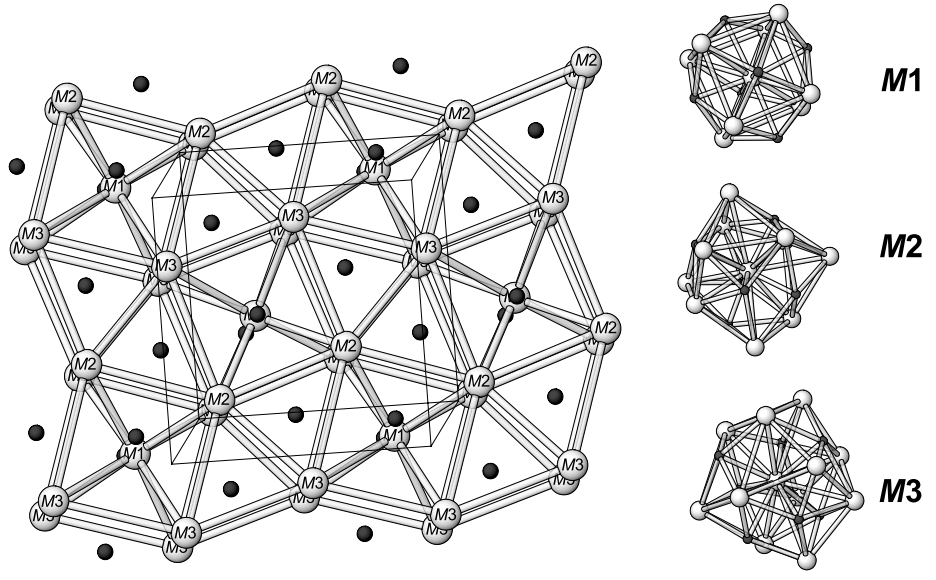

Fig. 3. The crystal structure type Sm_5Ge_4 adopted by $Hf_{5-x}Nb_xGe_4$ [26] and $Zr_{2+x}Ta_{3-x}Ge_4$ [24]; projection along [010]; metal atoms: bright spheres; sulfur atoms: small dark spheres; metal–metal bonds up to a distance of 4.0 Å are shown as sticks

Table 2. Site occupations of various M_5Ge_4 compounds determined by X-ray diffraction

Compound	Occupation at site			Reference
	*M*1	*M*2	*M*3	
$Zr_{3.98}Ta_{1.02}Ge_4$ (*tP*36)	0.41 Zr/0.59 Ta	0.79 Zr/0.21 Ta	1.00 Zr	[24]
$Zr_{3.90}Ta_{1.10}Ge_4$ (*mP*18)	0.36 Zr/0.64 Ta	0.77 Zr/0.23 Ta	1.00 Zr	[24]
$Zr_{3.13}Ta_{1.87}Ge_4$ (*oP*36)	0.10 Zr/0.90 Ta	0.50 Zr/0.50 Ta	1.00 Zr	[24]
$Zr_{2.29}Ta_{2.71}Ge_4$ (*oP*36)	1.00 Ta	0.17 Zr/0.83 Ta	0.97 Zr/0.03 Ta	[24]
$Hf_{4.45}Nb_{0.55}Ge_4$ (*oP*36)	0.58 Hf/0.42 Nb	0.94 Hf/0.06 Nb	1.00 Hf	[26]
$Hf_{3.40}Nb_{1.60}Ge_4$ (*oP*36)	0.15 Hf/0.85 Nb	0.62 Hf/0.38 Nb	1.00 Hf	[26]
$Hf_{2.28}Nb_{2.72}Ge_4$ (*oP*36)	0.05 Hf/0.95 Nb	0.21 Hf/0.79 Nb	0.91 Hf/0.09 Nb	[26]
$Hf_{1.36}Nb_{3.64}Ge_4$ (*oP*36)	1.00 Nb	1.00 Nb	0.68 Hf/0.32 Nb	[26]

blocks (bcc-fragments and trigonal prisms) and have three independent metal sites showing the same principal coordination arrangement [24].

Site occupation factors of different ternary compositions in the various M_5Ge_4 compounds obtained by refinement of X-ray single-crystal and powder data are listed in Table 2. As these data combine different metal pairs (Ta/Zr and Nb/Hf) they allow better insight into the amount to which the different possible driving forces for site preferences contribute to the fractional occupation adopted. Extended *Hückel* calculations show that the cumulated *M*–*M* *M*OPs are always the highest for the *M*1 position and the lowest for the *M*3 position of the different ternary phases [24]. The site volume (which is another possible driving force for differentiation) may be represented by the *Dirichlet* domains calculated using the program DIDO [27]. For the compounds listed in Table 2 the relative order of site volumes is $V(M1)<V(M2)<V(M3)$ [24, 26].

For the pair Zr/Ta this means that the 5*d* element Ta is predicted to favor the *M*1 site whereas the 4*d* element *Zr* should preferably occupy the *M*3 sites for optimized total *M*–*M* bonding. Size considerations (*Pauling* radii for Ta 134 pm, Zr 145 pm) yield an identical conclusion: the *M*1 position with the smallest site volume should be preferably occupied by the smaller Ta atoms whereas Zr should prefer the largest position *M*3. In the case of the metal pair Hf/Nb the optimization of *M*–*M* bonding interactions and size considerations leads to opposite conclusions regarding the predicted site preferences in $Hf_{5-x}Nb_xGe_4$. *M*–*M* bonding interactions would favor the preferential occupation of *M*1 by Hf as the 5*d* element whereas *Pauling* radii (Hf 144 pm, Nb 134 pm) point to a preferential occupation of the smaller Nb-atom on the site *M*1. Experimental values listed in Table 2 clearly show that geometrical factors connected with the site volumes outweigh *M*–*M* bonding interaction effects. This conclusion is in good agreement with observations in other DFSO-stabilized compounds which show that size effects generally overrule differences in *M*–*M* bonding capabilities [2].

A different approach to utilize electronic structure calculations for the rationalization of site preferences follows the idea of population analysis which was reviewed by *Miller* [28]. Atomic orbital populations (AOPs, local densities of states) obtained by extended *Hückel* calculations on homonuclear model compounds can be employed to identify differences among crystallographically

independent sites. It was demonstrated successfully for molecular structures as well as for crystalline solids, that site preferences can be understood by the assumption, that the element with the higher affinity to electrons (represented, *e.g.*, by electronegativity) will preferably occupy the site with the higher atomic orbital populations [28]. This method was adopted to the analysis of site preferences in mixed early transition metal germanides. Due to the difference in the number of electrons of the two metals (Zr/Ta or Hf/Nb) mixed at the metal sites, a rigid band approximation has to be used for population analysis, *i.e.* the *Fermi* level was to be adapted to the number of electrons actually present at a certain ternary composition. This approximation could be validated repeatedly by performing the same calculation on a binary group 4-group 5-compound and comparing the resulting electronic structure. According to the principles of population analysis, the more electron-rich group 5 metals Ta and Nb should preferably occupy the sites with the higher AOPs. Our calculations show, that this prediction was valid for all investigated M_5Ge_4 (Zr/Ta as well as Hf/Nb) compounds listed in Table 2 and also for the compound $Zr_xTa_{11-x}Ge_8$ which does not have close structural relations to the M_5Ge_4 phase bundle [25]. A plot of the atomic orbital population *versus* site fraction of the group 5 element (Ta or Nb) is shown in Fig. 4. Although the graph includes different structures and stoichiometries as well as different metal pairs, and although the corresponding AOP values were calculated on different hypothetic binaries ($Ta_{11}Ge_8$, Hf_5Ge_4, Zr_5Ge_4, etc.) [24–26] and thus with different sets of *Hückel* parameters, the correlation of data is surprisingly consistent.

A large number of ternary chalcogenides and pnictides of the early transition metals stabilized by DFSO as well as partially ordered solid solutions have been reported over the last decades [2]. Among them are a number of mixed group 4/5/6 compounds which allow to test the benefits and limits of population analysis on a broader basis. This group includes a number of phosphides like $Hf_{1+x}Mo_{1-x}P$ [11],

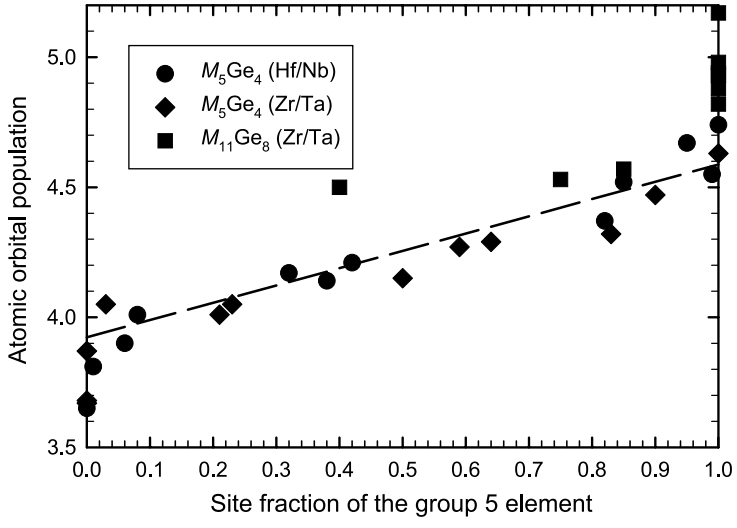

Fig. 4. Atomic orbital populations for various Hf/Nb and Zr/Ta germanides plotted *versus* experimentally observed site fractions at crystallographically independent lattice sites; each data point corresponds to a particular crystallographic site

$Hf_{5.08}Mo_{0.92}P_3$ [12], $Hf_5Nb_5Ni_3P_5$ [19], and the kappa phase $Hf_{9.29}Mo_{3.71}P$ [29] as well as arsenides like $Ti_{3.7}Mo_{1.3}As_3$ [17] and $Zr_{1-x}V_{1+x}As$ [15], the antimonides $(Zr, V)_{11}Sb_8$ and $(Zr, V)_{13}Sb_{10}$ [14], and the sulfide $Cr_{0.96}Ta_{5.04}S$ [30].

The corresponding extended *Hückel* calculations were performed in the present study using the CAESAR program package [31]. Where available, *Slater* coefficients and orbital energies used in the calculations were taken directly from the papers reporting on the respective compounds, otherwise standard sources were used and the orbital energies of the metals were obtained by solid state charge iteration. As the list of compounds tested combines a rather inhomogeneous group of structures, stoichiometries, and chemical compositions, it was decided to normalize the numerical values of the atomic orbital populations obtained in the calculations in order to get comparable values. This was done by using the average atomic orbital population of all metal sites of a certain structure at the *Fermi* levels of the hypothetical binary compounds as zero (for the electron-poor metal) and one (for the electron-rich metal) and normalizing the obtained numerical values for the atomic orbital populations at the *Fermi* level of the ternary compound accordingly. The resulting plot of these ''reduced'' atomic orbital populations *versus*

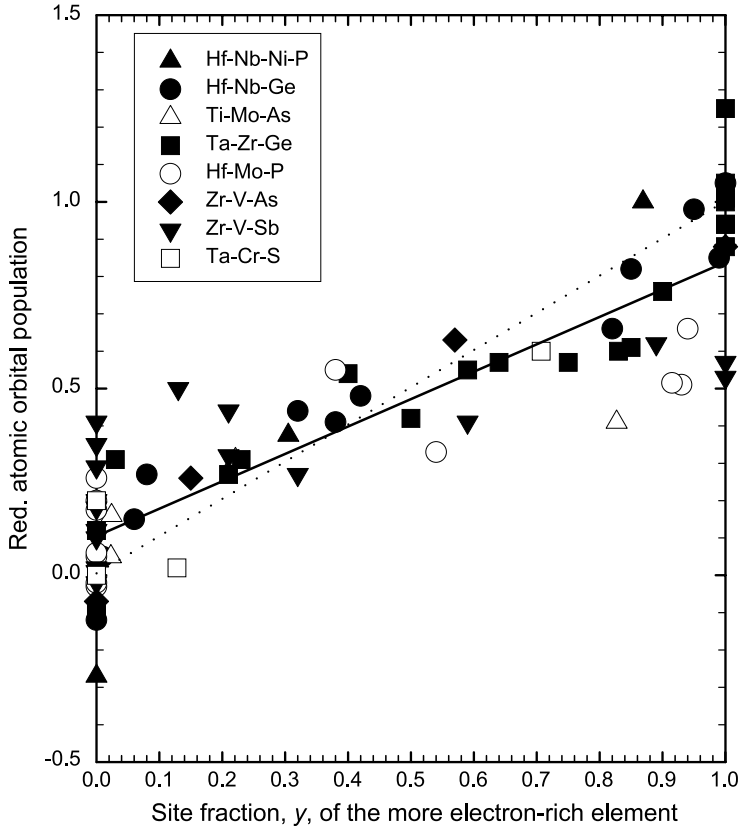

Fig. 5. Normalized atomic orbital populations calculated for 19 different ternary early transition metal compounds plotted *versus* experimentally observed site fractions at crystallographically independent lattice sites; the site fraction y is given for the electron-richer element of the respective metal pair

experimental values for site fractions y of the electron-rich metal of the respective metal pair is shown in Fig. 5. The plot includes experimental data from 19 different compounds in the ternary systems shown in the legend of the graph. The least square fit of all data points is shown as solid line.

The graph shows a clear qualitative relation between the site fraction at a certain lattice site and the corresponding AOP calculated for the same site. As expected the sites with the higher AOP are preferably occupied with the more electron-rich metal of the corresponding pair. Population analysis thus turns out to be a valuable prediction tool. It proved to provide a correct qualitative prediction of site preferences for a large number of early transition metal compounds with very different crystal structures, stoichiometries, and chemical compositions. The approach can be used for a much larger group of compounds than considerations based on metal–metal bonding interactions; i.e. compounds with metal pairs from different groups and also with metal pairs from the same group showing large enough difference in their electronegativity as it was demonstrated for the pair Hf/Ti by *Köckerling* and *Canadell* [32]. The relatively simple extended *Hückel* calculations can be performed in a reasonable time scale even for very large crystal structures (as they often occur in early transition metal – main group compounds) which would not be easily accessible for more sophisticated first principle calculations which are the main theoretical tool for site preference prediction for simpler structure types like the CsCl-type structure (*e.g.* Ref. [33]) or the Cu_3Au-type structure (*e.g.* Ref. [34]).

Thermodynamic Aspects

The solid solution phase $Hf_{5-x}Nb_xGe_4$ was used to discuss the thermodynamics of fractional site occupation in more detail [26]. The phase combines a large ternary

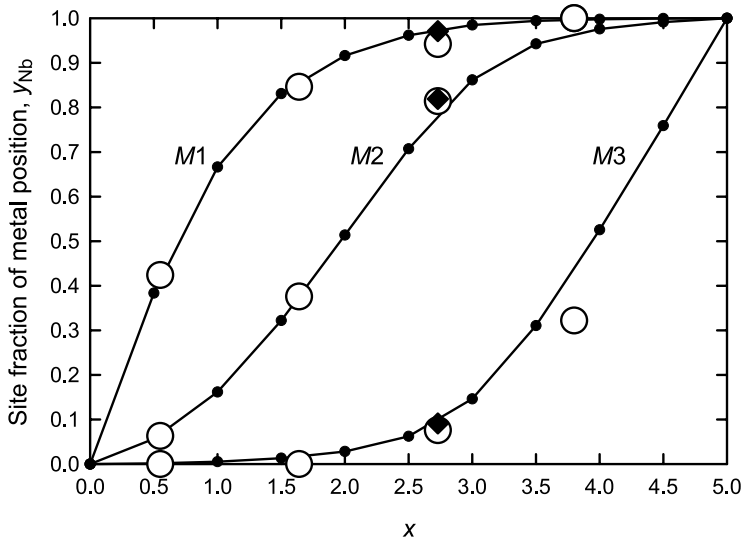

Fig. 6. Fractional site occupation at the three metal positions *M*1, *M*2, *M*3 in the partially ordered solid solution phase $Hf_{5-x}Nb_xGe_4$ as a function of composition; experimental data from powder diffraction (circles) and single crystal XRD (diamonds); the solid line corresponds to the prediction of the thermodynamic model

composition range ($0 \leq x \leq 3.8$) with strong site preferences leading to an almost stepwise substitution mechanism between Hf and Nb at the three metal sites of the structure. Experimental data of the Nb site fractions, y_{Nb}, at the three metal sites *M*1, *M*2, and *M*3 as a function of the composition parameter x in the formula $Hf_{5-x}Nb_xGe_4$ are shown graphically in Fig. 6.

The observed substitution mechanism reflects differences in the partial *Gibbs* energies of Nb and Hf at the three metal sites *M*1, *M*2, and *M*3. The experimental data for site occupations were used to determine the corresponding thermodynamic properties by the application of the compound energy model described by *Sundman* and *Ågren* [35]. According to the crystal structure of $Hf_{5-x}Nb_xGe_4$, a four sublattice model $(Hf, Nb)_{0.111}(Hf, Nb)_{0.222}(Hf, Nb)_{0.222}Ge_{0.445}$ was used. The first sublattice corresponds to the (4*c*) site *M*1, the second and third sublattice to the (8*d*) sites *M*2 and *M*3, and the fourth sublattice combines all three Ge-sites of the orthorhombic structure (two 4*c* and one 8*d* site). A total number of eight hypothetical ordered ''compounds'' (end members) were defined which may be written as (Hf:Hf:Hf:Ge), (Nb:Hf:Hf:Ge), (Hf:Nb:Nb:Ge), *etc*. in short notation. In order to reduce the number of parameters some simplifications were applied: 1) optimization for only one temperature ($T = 1400°C$) corresponding to the annealing temperature of the samples; 2) the *Gibbs* energy of the only physically existing end member (Hf:Hf:Hf:Ge) = Hf_5Ge_4 ($\Delta G = -55\,kJ\,mol^{-1}$ [26]) was taken as a reference state; 3) unique values for *Gibbs* energies were only given for three of the end members containing one sublattice filled with Nb (Nb:Hf:Hf:Ge), (Hf:Nb:Hf:Ge), and (Hf:Hf:Nb:Ge) and the others were described as combinations of these. The *Gibbs* energy of one mole of the compound was then formulated corresponding to the compound energy model and optimized values for the *Gibbs* energies of the unique end members (functioning as model parameters) were obtained by comparison of the resulting site fractions with the experimental values (for details compare Ref. [26]). The resulting curves for the variation of site occupations at *M*1, *M*2, and *M*3 with the composition according to the optimized model parameters are shown in Fig. 6 as solid curves and fit very well with the experimental data. The optimized values for the *Gibbs* energies of the unique end members relative to Hf_5Ge_4 (Hf:Hf:Hf:Ge) are $-2.8\,kJ\,mol^{-1}$ for (Nb:Hf:Hf:Ge), $+7.4\,kJ\,mol^{-1}$ for (Hf:Nb:Hf:Ge), and $+27.4\,kJ\,mol^{-1}$ for (Hf:Hf:Nb:Ge). The exchange of Hf by Nb is thus energetically favorable at the position *M*1, slightly destabilizing at the position *M*2, and strongly destabilizing at the position *M*3 yielding the equilibrium distribution of Nb and Hf shown in Fig. 6 for the temperature of 1400°C.

It is worth to consider the consequences of a change in temperature to the distribution equilibrium observed in the solid solution phase $Hf_{5-x}Nb_xGe_4$. Whereas annealing at higher temperature obviously will yield a higher weight of the ideal configuration entropy term and thus a more even distribution of the metals at the three lattice sites, the opposite will be true for the equilibrium distribution at lower temperatures and the ordering tendencies within $Hf_{5-x}Nb_xGe_4$ will finally end in the decomposition of the complete solid solution into stability islands. These will probably occur around the compositions of the most stable end members Hf_4NbGe_4 (Nb:Hf:Hf:Ge) and $Hf_2Nb_3Ge_4$ (Nb:Nb:Hf:Ge) with *Gibbs* energies relative to Hf_5Ge_4 of -2.8 and $+4.6\,kJ\,mol^{-1}$, respectively. The integral *Gibbs* energy of the solid solution phase $Hf_{5-x}Nb_xGe_4$ at 1400°C as derived from the

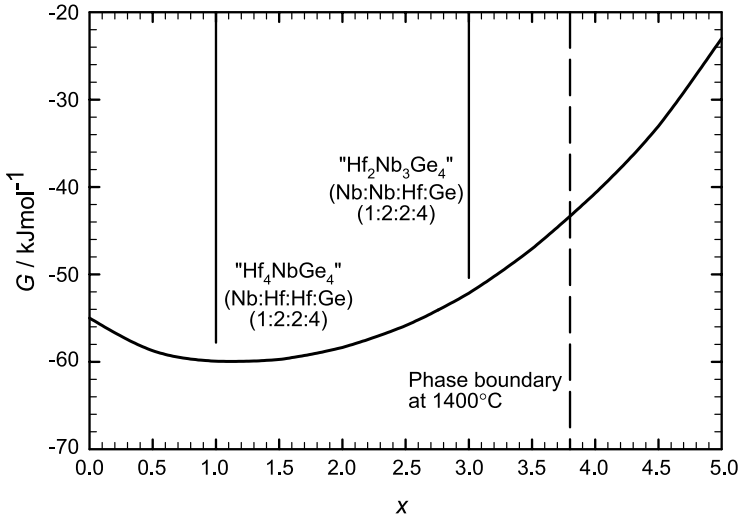

Fig. 7. Integral *Gibbs* energy of $Hf_{5-x}Nb_xGe_4$ as a function of composition at 1400°C for 1 mol of atoms according to the model applied in Ref. [26]; the solid lines show the most stable ''end members'' used in the model

thermodynamic model is shown in Fig. 7 together with the *Gibbs* energy of these two (hypothetical) ordered end members.

At this point it is interesting to take a closer look at the other ternary compounds adopting the same structure type (Sm_5Ge_4-type, *oP*36, *Pnma*). This structure type is quite common for binary intermetallics and roughly 50 binary compounds with the composition R_5A_4 with $R =$ rare earth and $A =$ Si, Ge, Pb, Rh, Ir, Pt, Au are listed in *Pearson*'s Handbook of crystallographic data [36]. An ordered ternary variant of this structure type which is sometimes referred to as $Ce_2Sc_3Si_4$-type [37] was found to exist in many ternary systems like, *e.g.*, the series $R_2Nb_3Ge_4$ ($R =$ rare earth) [38], $U_2Nb_3Ge_4$ [39], $Sc_2V_3Ge_4$, $Sc_2Nb_3Ge_4$, $Sc_2Nb_3Si_4$, and $Sc_2Mo_3Si_4$ [40]. In this compounds the lanthanide or actinide occupies the position *M*3 and the transition metal the positions *M*1 and *M*2 leading to the same atomic arrangement as in the end member (Nb:Nb:Hf:Ge) of our model. Additionally, a different ternary variant of Sm_5Ge_4 has been reported in Tm_4LiGe_4 [41] where Tm occupies the positions *M*2 and *M*3 whereas Li occupies the *M*1 position corresponding to the atomic arrangement in the end member (Nb:Hf:Hf:Ge) of our model. The existing ternary ordered variants of Sm_5Ge_4 thus correspond to either of the two most stable end members of the partially ordered solid solution $Hf_{5-x}Nb_xGe_4$ predicted to form the cores of stability islands at lower temperatures. The observation of an extended solid solution on the one side and reported ordered compounds on the other side, naturally raises the question whether it is possible to determine the intermediate state of partially disordered $Ce_2Sc_3Si_4$-type and Tm_4LiGe_4-type stability islands. In fact, hints for such behavior have been found in the system Sc–Pr–Si, where two separate compositions with Sm_5Ge_4-type structure have been reported [42]. One of them, $Sc_3Pr_2Si_4$ corresponds to the ordered $Ce_2Sc_3Si_4$-type, whereas the other, $Sc_{1.26}Pr_{3.74}Si_4$ has the refined site occupations *M*1: 0.35 Pr + 0.65 Sc, *M*2: 0.695 Pr + 0.305 Sc,

*M*3: 1.00Pr. This composition probably corresponds to the scandium-rich solid solubility limit of a stability island around $ScPr_4Si_4$, however, a systematic investigation along the M_5Si_4 section regarding the extent of this phase was not performed. Given the fact that the study of the Sc–Pr–Si system was performed on samples annealed at the low temperature of 600°C [39], it may well be that the two separate phase fields form a common phase field comparable to ternary $Zr_{2+x}Ta_{3-x}Ge_4$ [24] at elevated temperatures.

Conclusions

Partial ordering and differential fractional site occupation in transition metal compounds is probably a much more common phenomenon than generally perceived and thus deserves attention. Especially in the context of thermodynamic modeling of phase diagrams the knowledge of site preferences in crystal structure types which form solid solutions is crucial for the selection of correct and reliable sublattice models. It was demonstrated that the method of population analysis using extended *Hückel* calculations on binary structure prototypes allows the qualitative prediction of site preferences for a given metal pair. These predictions will be especially reliable when combined with size considerations. Furthermore, an estimation of thermodynamic driving forces can be obtained by the application of a simple thermodynamic model to a set of site fraction data determined experimentally from X-ray diffraction. This emphasizes the possibility to employ high quality structural results for thermodynamic assessments of multicomponent systems. Last but not least, the growing number of new ternary compounds synthesized in M–M'–A systems shows that an explorative synthesis of such compounds may be guided by considerations related to the principles of the differential fractional site occupation concept.

Acknowledgements

The author thanks Prof. *Herbert Ipser* for many helpful discussions. Financial support from the Austrian Science Foundation FWF, project number P16946, is gratefully acknowledged.

References

[1] Franzen HF (1978) Prog Solid State Chem **12**: 1
[2] Kleinke H (2001) Trends in Inorg Chem **7**: 135
[3] Yao X, Franzen HF (1990) J Solid State Chem **86**: 88
[4] Yao X, Franzen HF (1991) Z Anorg Allg Chem **598**: 353
[5] Yao X, Franzen HF (1991) J Amer Chem Soc **113**: 1426
[6] Yao X, Miller GJ, Franzen HF (1992) J Alloys Comp **183**: 7
[7] Debus S, Harbrecht B (2002) J Alloys Comp **338**: 253
[8] Harbrecht B (1989) Z Kristallogr **186**: 119
[9] Marking GA, Franzen HF (1993) Chem Mater **5**: 678
[10] Marking GA, Young VG, Franzen HF (1996) J Alloys Comp **241**: 98
[11] Miller GJ, Cheng J (1995) Inorg Chem **34**: 2962
[12] Cheng J, Franzen HF (1996) J Solid State Chem **121**: 362
[13] Kleinke H, Franzen HF (1998) J Solid State Chem **136**: 221

[14] Kleinke H (1999) J Mater Chem **9**: 2703
[15] Dashjav E, Lee CS, Kleinke H (2002) J Solid State Chem **169**: 96
[16] Kleinke H (2000) J Am Chem Soc **122**: 853
[17] Lee CS, Dashjav E, Kleinke H (2002) J Alloys Comp **338**: 60
[18] Kleinke H (1999) Inorg Chem **38**: 2931
[19] Kleinke H, Franzen HF (1997) J Am Chem Soc **119**: 12824
[20] Franzen HF, Köckerling M (1995) Prog Solid State Chem **23**: 265
[21] Emsley J (1989) The Elements. Clarendon Press, Oxford
[22] Yao X, Marking G, Franzen HF (1992) Ber Bunsenges Phys Chem **96**: 1552
[23] Pauling L (1948) The Nature of the Chemical Bond. Cornell University Press, NY
[24] Richter KW, Franzen HF (2000) J Solid State Chem **150**: 347
[25] Richter KW, Flandorfer H, Franzen HF (2002) J Solid State Chem **167**: 517
[26] Richter KW, Picha R, Ipser H, Franzen HF (2003) Solid State Sci **5**: 653
[27] Koch E, Fischer W (1996) Z Kristallogr **211**: 251
[28] Miller GJ (1998) Eur J Inorg Chem **5**: 523
[29] Hårsta A (1982) Acta Chem Scand **A36**: 535
[30] Harbrecht B, Franzen HF (1987) Z anorg allg Chem **551**: 74
[31] Ren J, Liang W, Whangbo MH (1998) CAESAR Software, North Carolina State University
[32] Köckerling M, Canadell E (2000) Inorg Chem **39**: 4200
[33] Song Y, Yang R, Li D, Hu ZQ, Guo ZX (2000) Intermetallics **8**: 563
[34] Ruban AV, Skriver HL (1997) Phys Rev B **55**: 856
[35] Sundman B, Ågren J (1981) J Phys Chem Solids **42**: 297
[36] Villars P, Calvert LD (eds) (1991) Pearson's Handbook of Crystallographic Data, 2nd ed. ASM
[37] Mokra IR, Bodak OI, Gladyshevskii EI (1979) Sov Phys Crystallogr **24**: 729
[38] Le Bihan T, Hiebl K, Rogl P, Noël H (1996) J Alloys Comp **235**: 80
[39] Le Bihan T, Noël H, Rogl P (1994) J Alloys Comp **213**: 540
[40] Kotur BYa, Bodak OI, Zavodnik VE (1986) Sov Phys Crystallogr **31**: 513
[41] Pavlyuk VV, Bodak OI, Zavodnik VE (1990) Dopov Akad Nauk Ukr RSR Ser B **N12**: 29
[42] Kotur BYa, Banakh OE, Cerny R, Pacheco Espejel JV (1997) J Alloys Comp **260**: 157